Synergy between Individual TNF-Dependent Functions Determines Granuloma Performance for Controlling *Mycobacterium tuberculosis* Infection[1]

J. Christian J. Ray,[2]* JoAnne L. Flynn,[†] and Denise E. Kirschner[3]*

Mycobacterium tuberculosis* is one of the world's most deadly human pathogens; an integrated understanding of how it successfully survives in its host is crucial to developing new treatment strategies. One notable characteristic of infection with *M. tuberculosis* is the formation of granulomas, aggregates of immune cells whose structure and function may reflect success or failure of the host to contain infection. One central regulator of host responses to infection, including granuloma formation, is the pleiotropic cytokine TNF-α. Experimental work has characterized roles for TNF in macrophage activation; regulation of apoptosis; chemokine and cytokine production; and regulation of cellular recruitment via transendothelial migration. Separating the effects of these functions is presently difficult or impossible in vivo. To this end, we applied a computational model to understand specific roles of TNF in control of tuberculosis in a single granuloma. In the model, cells are represented as discrete entities on a spatial grid responding to environmental stimuli by following programmed rules determined from published experimental studies. Simulated granulomas emerge as a result of these rules. After confirming the importance of TNF in this model, we assessed the effects of individual TNF functions. The model predicts that multiple TNF activities contribute to control of infection within the granuloma, with macrophage activation as a key effector mechanism for controlling bacterial growth. Results suggest that bacterial numbers are a strong contributing factor to granuloma structure with TNF. Finally, TNF-dependent apoptosis may reduce inflammation at the cost of impairing mycobacterial clearance.** ***The Journal of Immunology, **2009, 182: 3706–3717.**

Tuberculosis (TB)[4] kills more people per year than any other single infectious disease. Infection by its causative agent, *Mycobacterium tuberculosis* (Mtb), results in active disease in only a minority of cases (~10%); the majority of infections are controlled and clinically silent, although the host often remains infected (reviewed in Ref. 1).

The classic feature of pulmonary Mtb infection arises as a result of the immune response, in which aggregates of immune cells and bacteria, called granulomas, form in the lungs. In humans and nonhuman primates with latent pulmonary infection, granulomas form as well-circumscribed masses in the lung parenchyma comprised of resting, infected, and activated macrophages with a characteristic cuff of T cells on the periphery (e.g., Refs. 2 and 3) and a caseous necrotic center (4). Macrophages within a granuloma have dual roles in Mtb infection: they are the primary mechanism for Mtb containment and the preferred location for bacterial growth. During infection, there are often multiple and different types of granulomas within the lung; each could have a different outcome depending on local environment. At the level of a single granuloma, macrophages may fail to control infection, leading to necrotic granulomas harboring large numbers of bacteria within macrophages (3). However, the relationship between bacterial control in a single granuloma and the outcome of infection at the level of the entire host are not well established (3).

Type 1 adaptive immunity is required to control infection at the host level (5). Activated T cells migrate to the site of infection and act as immune effectors. We distinguish three primary T cell types based on their effector function (cf Ref. 6). Proinflammatory T cells ($CD4^+$ or $CD8^+$) provide macrophage-activating cytokines (e.g., IFN-γ), whereas CTLs (predominantly $CD8^+$) provide cytolytic functions to control infection (reviewed in Ref. 1). A third T cell class, regulatory T cells (T_{reg}; reviewed in Ref. 7), are present in mouse (8) and human (9) Mtb infections, and may prevent efficient Mtb clearance by immune responses (10, 11), or may modulate local responses to control pathology. T_{reg} are $CD4^+Foxp3^+$ cells that comprise ~5–10% of all $CD4^+$ T cells (12, 13). They suppress the action of proinflammatory T cells (14) through poorly understood mechanisms that may occur by cell contact, secretion of immunosuppressive cytokines (15), or both.

The proinflammatory cytokine TNF-α (TNF) is a central, multifaceted contributor to the immune response in Mtb infection produced by activated macrophages and proinflammatory T cells (16–20). The role of TNF is of clinical interest due to the

*Department of Microbiology and Immunology, University of Michigan Medical School, Ann Arbor, MI 48109; and [†]Department of Microbiology and Molecular Genetics, University of Pittsburgh School of Medicine, Pittsburgh, PA 15261

Received for publication July 15, 2008. Accepted for publication January 5, 2009.

The costs of publication of this article were defrayed in part by the payment of page charges. This article must therefore be hereby marked *advertisement* in accordance with 18 U.S.C. Section 1734 solely to indicate this fact.

[1] This work was supported by National Institutes of Health Grants HL68526 (to D.E.K. and J.L.F.), NO1 AI50018 (to J.L.F. and D.E.K.), HL72682 (to D.E.K.), and LM00902701 (to D.E.K. and J.L.F.); the F.G. Novy Fellowship (to J.C.J.R.); and the Ellison Foundation (to J.L.F.).

[2] Current address: Department of Bioengineering, Rice University, Houston, TX 77251.

[3] Address correspondence and reprint requests to Dr. Denise E. Kirschner, Department of Microbiology and Immunology, University of Michigan Medical School, 6730 Medical Science Building II, Ann Arbor, MI 48109-0620. E-mail address: kirschne@umich.edu

[4] Abbreviations used in this paper: TB, tuberculosis; ABM, agent-based model; M_a, activated macrophage; M_{ci}, chronically infected macrophage; M_i, infected macrophage; M_r, resting macrophage; Mtb, *Mycobacterium tuberculosis*; T_{move}, probability of T cell movement onto an occupied location; s_{TNF}, overall rate of TNF production; T_{reg}, regulatory T cell.

www.jimmunol.org/cgi/doi/10.4049/jimmunol.0802297

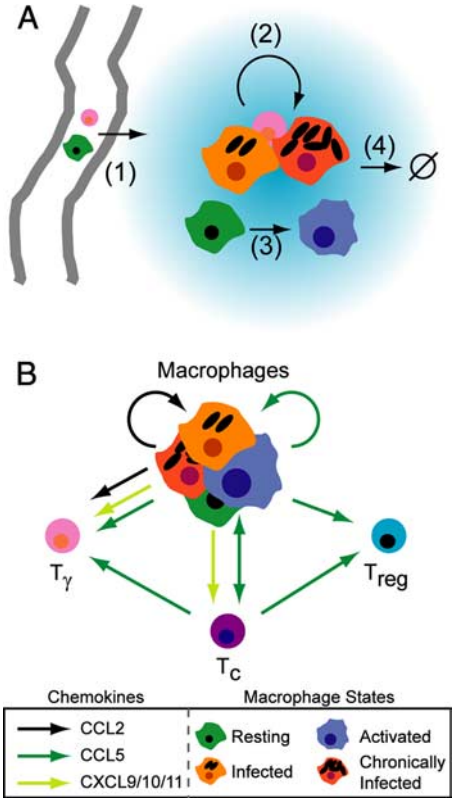

FIGURE 1. Models of molecular signaling networks that affect granuloma formation during infection with Mtb. *A*, TNF (blue gradient) is an immunological effector with multiple roles. *1*, TNF-dependent enhancement of transendothelial migration of monocytes and T cells to the lung parenchyma occurs via up-regulation of endothelial adhesion molecules. *2* and *3*, TNF-dependent activation of macrophages in concert with IFN-γ stimulates chemokine production and bacterial killing. *4*, TNF-dependent apoptosis, a second pathway for mycobacterial killing. *B*, Model of the chemokine network induced during infection with Mtb. CXCL9/10/11 are α-chemoattractants that bind the same chemokine receptor (CXCR3); CCL2 binds CCR2; CCL5 binds CCR5. T_γ are proinflammatory Th1 cells. T_c are CTLs.

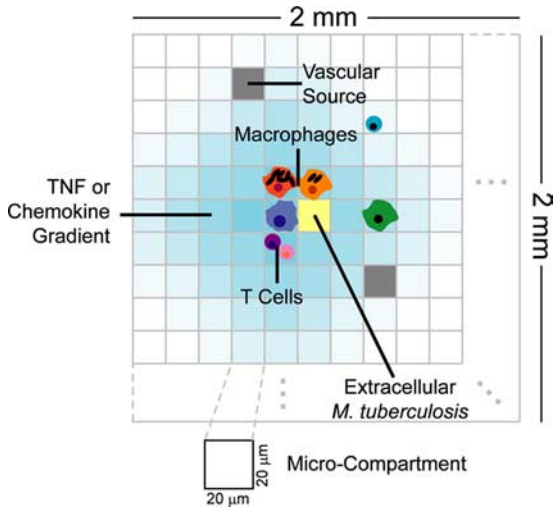

FIGURE 2. Structure of the ABM environment. A section of the 100 × 100 grid of microcompartments that represents a 2 mm × 2-mm section of lung tissue. Discrete entities include macrophages and T cells. TNF, chemokines, and extracellular Mtb are represented as continuous entities. Each microcompartment can contain either one macrophage or up to two T cells along with extracellular bacteria, TNF, and chemokines. A percentage of randomly chosen microcompartments is designated as vascular sources that allow new macrophages and T cells to be recruited to the grid by chemokines and TNF.

association of anti-inflammatory TNF-blocking drugs with reactivation of latent TB in humans (21, 22). TNF is also necessary for Mtb containment in mouse models (16). TNF gene-disrupted or neutralized mice have disorganized granulomas in Mtb infections (17), underscoring the link between granuloma structure and effective containment of infection.

TNF has multiple immunological functions during infection with Mtb (Fig. 1*A*). TNF has a direct role in immune cell recruitment via up-regulation of endothelial adhesion molecules (23), facilitating transendothelial migration of immune cells to the site of infection. TNF regulates production of chemokines by macrophages (24, 25); chemokines can further induce transendothelial migration (reviewed in Ref. 26) and coordinate recruitment (reviewed in Ref. 27) of immune cells within the tissues. TNF activates macrophages in conjunction with the cytokine IFN-γ (28–30); such activated macrophages can kill intracellular mycobacteria. TNF can also induce necrotic or apoptotic cell death in macrophages (31) that is promoted by Mtb infection (32). Fig. 1*A* summarizes these effects.

The effects of TNF in Mtb granuloma formation are most likely related to the chemokine network induced during infection. We have identified a simplified model of chemokines based on three classes that affect recruitment of macrophages and T cells to the granuloma via binding of appropriate chemokine receptors on the cell surface (Fig. 1*B*). The α-chemoattractant class (CXCL9, 10, and 11; formerly monokine induced by IFN-γ, IFN-γ-inducible protein-10, and IFN-inducible T cell α-chemoattractant, respectively) binds chemokine receptor CXCR3 on proinflammatory $CD4^+$ and $CD8^+$ T cells (33), but not regulatory T cells (34). CCL2 (formerly MCP-1) binds CCR2 on macrophages (35) and proportions of proinflammatory T cell populations (36). CCL5 (formerly RANTES) binds CCR5 on macrophages and T cells, and is involved in migration of regulatory T cells to the site of other infections (37), although this has not been demonstrated for Mtb.

Each of the four roles of TNF (cellular migration, induction of chemokine/TNF secretion, macrophage activation, and apoptosis) may contribute separately to establishing and maintaining control of Mtb infection at the level of a single granuloma. Currently, it is impossible to study these separate TNF functions using in vitro or in vivo models. In this study, we use a specific type of computational model known as an agent-based model (ABM) to study the contributions of these immune effectors on granuloma formation (illustrated in Fig. 2). The power of this approach lies in the emergence of behaviors that arise from interactions between agents that would otherwise be impossible to know a priori. We build on our previously described ABM (38), which predicted the emergence of two-dimensional spherical structures (granulomas) without any rules specifying such spatial behavior to occur. We now incorporate various functions of TNF, different T cell classes, and a simple chemokine network. This type of model, which combines spatial and temporal behaviors, is particularly suited to the investigation of granulomas due to the representation of cells, cytokines, and bacteria, allowing tractable analysis of each factor independently or in combination. Analysis of an ABM reveals the specific contributions of TNF functions, alone and in combination, to control of Mtb infection and granuloma structure at the level of a single granuloma.

Materials and Methods

Supplemental methods, results, and time-lapse movies are available at http://malthus.micro.med.umich.edu/lab/movies/Granuloma2009/.

Hybrid ABM

The model presented in this study is an extension of a previous ABM that captured cellular interactions leading to granuloma formation during infection with Mtb (38). The model is considered hybrid because we incorporated both discrete entities (cells) and continuous entities (chemokines, TNF, and Mtb) that interact simultaneously. ABMs are developed based on four considerations: an environment, agents that reside there, the rules that describe the agents and their interactions, and the timescales on which events are defined.

The environment represents a 2 mm × 2-mm section of lung parenchyma as a 100 × 100-square two-dimensional lattice with individual microcompartments scaled to the approximate size of a single macrophage 20 μm in diameter (39). Discrete agents move on the lattice and respond to their environment based on rules reflecting known biological activities. Bacteria and effector molecules can reside anywhere on the lattice and undergo diffusion when appropriate.

Caseation represents inflammation of, and damage to, the lung parenchyma from macrophage cell death. We note a change of terminology to caseation from necrosis in previous work (38), because strict necrosis within the granuloma is now believed to be caused by substantial neutrophil infiltration and death, whereas caseation is most likely initiated by macrophage death (J. L. Flynn, unpublished data). In the ABM, caseation is defined to occur when a threshold number of activated or infected macrophage deaths take place in a microcompartment. A final environmental feature is designation of spaces as vascular sources.

We include two types of discrete agents in the model, as follows: macrophages and T cells. As previously (20, 38), macrophage agents are either resting (M_r, uninfected), infected (M_i; have taken up bacteria), chronically infected (M_{ci}; are unable to clear their intracellular bacterial load), or activated (M_a; can effectively kill bacteria). In contrast to our previous study (38), in which a single T cell class captured all cell behaviors, in this study we represent three distinct T cell subpopulations based on function, as follows: the T_γ class captures $CD4^+$ and $CD8^+$ proinflammatory T cells; T_c represent CTLs; and T_{reg} represent regulatory T cells. In this representation, all T cells in a particular class have identical function; this is simpler than in vivo, but we capture enough detail in this representation for a qualitative representation of known T cell effects.

In addition to the discrete entities, extracellular bacteria and diffusing effector molecules (CCL2, CCL5, CXCL9/10/11, and TNF) are agents (concentrations) that are tracked continuously over time. The chemokine model used in this study is a simplification that was chosen to include a ligand for each key chemokine receptor, while minimizing the distinct chemokine classes represented to save on computation.

Cells respond to signals in the surrounding environment according to rules that represent known activities in vivo. During simulations, each agent responds depending on its state. Examples of rules include uptake of bacteria, macrophage activation by T cells, secretion of cytokines and chemokines, etc. For a full list of rules, see Supplement 1.[5]

Computer simulations

At the beginning of a simulation, the grid has 105 randomly placed resident M_r that move randomly with no chemokine or cytokine present. Infection is initiated with one M_i, containing a single bacterium, placed at the center. We chose this inoculum because we assume a single inhalation event. We also compared our results using a single bacterium to one using a larger inoculum (15 bacteria within an infected macrophage). In that scenario, clearance of infection occurred less often, with different kinetics at early timepoints, but after 20 days the two infection trajectories and bacterial loads become similar from that point forward. Every 10 min of simulation time, positions and interactions between T cells and macrophages are updated, including recruitment of cells from vascular sources and secretion of TNF and chemokines. The landscape of molecular concentrations serves as the starting point for computing cytokine and chemokine diffusion for 10 min of simulation time. Cell states and interactions are then updated again, in the beginning of the next 10-min timestep in an asynchronous fashion, and the algorithm continues in this way for 200 days (2,880,000 6-s timesteps) of simulation time.

[5] The online version of this article contains supplemental material.

Parameter estimates and uncertainty and sensitivity analyses

It is difficult to estimate the rates and probabilities (parameters) of events occurring within the lung environment. We approximate parameter values in three ways: directly from available data, using uncertainty analysis, and model calibration with other data. Relative macrophage and T cell production were estimated from the literature (40–44). The macrophage CCL2 saturation point and detection threshold were estimated based on published data (45); T cell saturations are inferred from this. T_{reg} are more sensitive to CCL5 than T_γ or T_c cells (42, 46). The resting macrophage lifespan is based on (47), we assume, a lifespan 10-fold shorter for activated macrophages. The lifespan of a T cell is based on previous description (48). The delay of T cell infiltration is based on previous description (49).

Because absolute levels of chemokine production, saturation, etc., were not known, we estimated the relative effects using calibration. Chemokine diffusion is based on previous description (50). The initial number of macrophages represents ~1% coverage of the grid (38). The number of bacteria engulfed or killed by resting macrophages was chosen to be low, but nonzero. The killing of ingested bacteria by activated macrophages is related to the maximum number of intracellular Mtb that can exist in an infected macrophage before it is designated as chronically infected. N_{tact} is a guess based on physical interactions of several T cells around a single macrophage. Other parameter value estimates are discussed in supplemental material.

All other parameters not discussed above that are listed in Tables I and III were estimated using uncertainty analysis, with various parameters calibrated to ensure distinct outcomes between control and TNF-deletion cases. Parameters in Table II, including production, sensitivity and saturation thresholds, and effects on recruitment for all other chemokines, were defined to preserve a relative relationship with the CCL5 parameters (dependent parameters). Thus, when Table I parameters (independent parameters) vary, Table II parameters also vary because they are proportional.

Because not all parameters can be estimated from available data, it is necessary to use uncertainty and sensitivity methods to explore possible model outcomes using different parameter values. We have developed extensive methods for performing this analysis on ABMs and applied them in this study (see Ref. 51; for more details see Supplement 2). Simulations using uncertainty analyses yielded a wide range of different granuloma structures and bacterial numbers within the granulomas (supplementary Fig. S1). Data from humans and nonhuman primates with TB strongly support the existence of a diverse array of granuloma types even within a single host (4, 52).

Simulated deletion and depletion of TNF activities

To examine the effect of individual TNF activities on granuloma formation and maintenance, we performed virtual deletions and depletions of relevant parameters using a baseline parameter set that leads to control of infection (Tables I–III). Loss of activity was brought about by setting relevant probabilities to zero and/or raising relevant thresholds to an unattainable level. Virtual deletion refers to loss of the activity from the beginning of the simulation at the onset of infection. Virtual depletion refers to the loss of the activity after the establishment of a stable granuloma, 100 days postinfection. The timing of the depletion was determined by examining the results of sensitivity analysis and the baseline control scenario. Parameter sensitivities in the model stabilize by day 50 (cf, *Results*), suggesting that 100 days postinfection represents a reasonable time for an established, stable granuloma. Significant differences between outcome variables were determined with a mean difference test (Welch's approximate *t* test) for 15 repeated simulations of each single deletion or depletion, and for 10 repeated simulations in deletion or depletion of two or more TNF activities simultaneously (for details, see Supplement 2).

Simulations with bacterial levels fixed after 100 days postinfection

To control for the effects of bacterial growth on granuloma structure, we fixed total bacterial levels ($B_e + B_i$). Specifically, we simulated a baseline granuloma for 100 days and then fixed the total bacterial numbers to a constant level (2.75 ± 0.51 $\log_{10}$ Mtb) for the next 100 simulation days. This allowed exploration of the effects of TNF depletions without the confounding effects of bacterial growth. To attain a fixed Mtb population, all bacterial growth and death were prevented, with the effects of bacteria on host macrophages allowed to otherwise proceed normally. Upon exit of intracellular Mtb from macrophages due to cell

Table I. *Parameters varied for Latin hypercube sampling*

Parameter	Description[a]	Default	Range	Distribution	Varied in Focused Analysis?
α_{Bi}	Intracellular Mtb growth rate (per 10 min)	0.002	0.0002, 0.002	Uniform	No
α_{Be}	Extracellular Mtb growth rate (per 10 min)	0.001	0.00015, 0.015	Log-Uniform	No
p_k	Probability of M_r killing bacteria	0.015	0.01, 0.1	Uniform	No
T_{actm}	Probability of M_i activation by T_γ	0.05	0.0001, 0.1	Log-Uniform	No
M_{recr}	Probability of macrophage recruitment	0.075	0.01, 0.1	Uniform	No
T_{recr}	Probability of T cell recruitment	0.075	0.01, 0.1	Uniform	No
T_{move}	Probability of a T cell moving onto an occupied microcompartment	0.01	0.00001, 0.1	Log-Uniform	No
T_{rrecr}	Proportion of T_{reg} cells out of all T cells recruited	0.1	0.01, 0.2	Uniform	No
λ_c	Chemokine diffusion rate (cm^2 per 0.1 min)	6.27×10^{-7}	$1,7 \times 10^{-7}$	Uniform	No
δ_c	Chemokine degradation rate (per 0.1 min)	0.00123	0.0005, 0.0015	Uniform	No
r_T	Combined TNF/chemokine threshold for T cell recruitment at a vascular source[b]	1,000	$0.1{,}10 \times 10^4$	Log-Uniform	No
r_M	Combined TNF/chemokine threshold for M_r recruitment at a vascular source[b]	1,000	$0.1{,}10 \times 10^4$	Log-Uniform	No
s_{c5}	CCL5 production rate (molecules per 10 min)	7.5×10^4	$1{,}10 \times 10^4$	Uniform	No
s_{5m}	Macrophage CCL5 saturation threshold (molecules)	1.413×10^4	$1{,}100 \times 10^4$	Log-Uniform	No
τ_{5m}	Macrophage CCL5 threshold (molecules)	2×10^4	$1{,}100 \times 10^4$	Log-Uniform	No
λ_{TNF}	TNF diffusion rate (cm^2 per 0.1 min)	6.56×10^{-7}	$1,7 \times 10^{-7}$	Uniform	Yes
δ_{TNF}	TNF degradation rate (per 0.1 min)	0.0006	0.0001, 0.001	Uniform	Yes
s_{TNF}	TNF production rate (molecules per 10 min)	2.25×10^5	$1{,}100 \times 10^4$	Log-Uniform	Yes
p_{apopt}	Probability of TNF-induced apopt per 10 min interval	0.1	0.001, 0.2	Uniform	Yes
τ_{TNF}[c]	Macrophage TNF detection threshold (molecules)	7×10^5	$1{,}15 \times 10^5$	Uniform	Yes
r_{MTNF}	Effect of TNF on M_r recruitment[b]	150	10, 1000	Log-Uniform	Yes

[a] All probabilities are per 10-min interval.
[b] Nondimensional; cf II.3.iv-v. of the ABM rules (Supplement 1).
[c] τ_{TNF} was divided into separate thresholds for activation (τ_{TNFact}) and apoptosis ($\tau_{TNFapopt}$) in the focused analysis.

lysis or death, the bacteria were forced to deposit on the single microcompartment where the macrophage resided after day 100 (unlike other simulations, in which bacteria were distributed in the entire (Moore) neighborhood of a macrophage). This step prevents a biologically unrealistic scenario that could occur in which the bacteria are shuffled to the outside of the granuloma. Note that intracellular and extracellular Mtb quantities still changed in the simulations, but the total bacterial number was conserved.

Results

An ABM for dissection of granuloma structure and function

Computational models of the immune response to a pathogen can be deterministic (based on ordinary differential equations representing rates of change) or stochastic (based on probabilities of discrete agents and the rules governing their behavior). For the current investigation examining the contribution of various functions of TNF to granuloma structure and bacterial control in Mtb infection, we chose to use an ABM that is a hybrid model. This approach is appropriate because both spatial and temporal events must be considered when investigating the tuberculous granuloma. The ABM predicts the dynamics of Mtb infection at the level of a single granuloma.

To first identify variables that determine initial containment or maintenance of an established infection at the scale of a single granuloma, we established a reference parameter set (Tables I–III) using uncertainty and sensitivity analyses, as outlined in *Materials and Methods* and Supplement 2. The baseline simulations lead to stable bacterial numbers contained within the granuloma ($\sim 10^3$ total bacteria) up to 200 days postinfection (Fig. 3*A*, □). Repeated simulations show that the granuloma is organized with relatively tightly packed cells, predominantly uninfected macrophages (green agents in Fig. 3*B*), with T cell localization at the periphery of the granuloma (pink, purple, and light blue agents in Fig. 3*B*). The model is robust: for 15 repeated runs that established stable bacterial levels, all showed controlled infection with variable outcomes of granuloma structure (Supplement 3, Fig. S2*A* presents repeat simulations of the baseline scenario illustrating extent of variability).

Table II. *Parameter relationships constrained for analyses*

Parameter	Description	Value
s_{c2}	CCL2 production rate (molecules per 10 min)	s_{c5}
s_{c9}	CXCL9/10/11 production rate (molecules per 10 min)	$2*s_{c5}$
s_{2m}	Macrophage CCL2 saturation (molecules)	$10*s_{5m}$
τ_{2m}	Macrophage CCL2 threshold (molecules)	$0.1*t_{5m}$
$s_{2T\gamma}$	T_γ CCL2 saturation (molecules)	$10*s_{5m}$
$\tau_{2T\gamma}$	T_γ CCL2 threshold (molecules)	$0.1*t_{5m}$
$s_{5T\gamma}$	T_γ CCL5 saturation (molecules)	s_{5m}
$\tau_{5T\gamma}$	T_γ CCL5 threshold (molecules)	τ_{5m}
$s_{9T\gamma}$	T_γ CXCL9 saturation (molecules)	$10*s_{5m}$
$\tau_{9T\gamma}$	T_γ CXCL9 threshold (molecules)	τ_{5m}
s_{5Tc}	T_c CCL5 saturation (molecules)	s_{5m}
τ_{5Tc}	T_c CCL5 threshold (molecules)	τ_{5m}
s_{9Tc}	T_c CXCL9 saturation (molecules)	$10*s_{5m}$
τ_{9Tc}	T_c CXCL9 threshold (molecules)	τ_{5m}
s_{5Tr}	T_{reg} CCL5 saturation (molecules)	s_{5m}
τ_{5Tr}	T_{reg} CCL5 threshold (molecules)	$0.1*t_{5m}$
r_{M2}	Effect of CCL2 on M_r recr[a,b]	r_{MTNF}
r_{M5}	Effect of CCL5 on M_r recr[a,b]	$0.1*r_{MTNF}$
r_{TTNF}	Effect of TNF on T cell recr[a]	r_{MTNF}
r_{T9}	Effect of CXCL9 on T_γ, T_c cell recr[a,b]	$0.1*r_{MTNF}$
$r_{T\gamma 2}$	Effect of CCL2 on T_γ cell recr[a,b]	r_{MTNF}
r_{T5}	Effect of CCL5 on T_γ, T_c cell recr[a,b]	$0.1*r_{MTNF}$
r_{Tr5}	Effect of CCL5 on T_{reg} cell recr[a,b]	r_{MTNF}
$T_{\gamma recr}$	Proportion of T_γ cells recruited	$0.6*(1-T_{rrecr})$
T_{crecr}	Proportion of T_c cells recruited	$0.4*(1-T_{rrecr})$

[a] Nondimensional; cf II.3.iv-v. of the ABM Rules (Supplement 1).
[b] These parameters were held constant in the focused sensitivity analysis at the default value of r_{MTNF} given in Table I.

Table III. *Parameters not varied in uncertainty analysis*

Parameter	Description	Value	Reasoning
M_{init}	Number of resident macrophages	105	1
K_{be}	Carrying capacity of microcompartment for extracellular Mtb	220	2, 3
N_{rk}	Number of Mtb engulfed/killed by M_r	2	3
N_{phag}	Number of Mtb killed by M_a every 10 min	10	3
N_{tact}	Maximum T_γ number in Moore of M_i having effect	4	3
N_{caseum}	Number of M_a, M_i, and M_{ci} deaths for caseation	6	3
$t_{regT\gamma}$	T_γ inactivity time after T_{reg} interactions (min)	110	3
N_c	Number of Mtb for $M_i \rightarrow M_{ci}$ transition	10	3, 4
K_{bi}	Number of bacteria causing bursting	20	3, 4
M_{als}	Lifespan of M_a in days	10	5
T_{ls}	Lifespan of T cells in days	3	5
M_{rls}	Lifespan of M_r in days	100	5
T_{delay}	T cell recruitment delay in days	20	6
P_{kill}	Fraction Mtb killed by Fas/Fas ligand apoptosis	0.5	7
p_{Tk}	Probability of Fas/Fas ligand (TNF-independent) apoptosis by T cells	0.006	7
T_{ckmtb}	Probability of T_c killing Mtb in M_{ci} death	0.75	7
T_{ckmci}	Probability of T_c killing M_{ci}	0.95	7

1. Set to the reference number for containment to have identical initial conditions.
2. Set ~10-fold larger than the amount causing macrophage bursting. There is physical space for ~450 bacilli in one microcompartment (tightly packed), but lack of nutrients for growth limits this.
3. These parameters have integer values that cannot be continuously varied over at least 250 different values.
4. The same effect as varying this is captured by changing intracellular growth rate: the faster Mtb grow, the sooner the transition to chronic infection. If N_c is varied in say 5, 25, we should set $K_{bi} = 2*N_c$.
5. Relative lifespans are well known. Vary cell age between 0 and the maximum age, so changing these would have questionable relevance.
6. Many parameter sensitivities change before and after this time, so it was held constant, but multiple uncertainty analyses were performed to show the effect of this parameter.
7. Preliminary analysis revealed little effect for reasonable ranges. Thus, this was not varied to reduce the number of parameters varied.

Simulated infection with all parameters set to the control scenario, but lacking TNF (virtual TNF deletion) results in a granuloma that is irregular in shape, increased in size, and with widespread caseation (Fig. 3*C*). Bacterial numbers are significantly higher than in the baseline scenario (Fig. 3*A*, ▨: ~10^4 compared with 10^3; $p < 0.01$). Numbers of all macrophage and T cell populations in the model are significantly elevated in comparison with the baseline scenario within the first 20 days after infection (data not shown). Therefore, loss of TNF appears to impair early control of infection, resulting in more extensive immune cell infiltration; this corresponds to data from murine models of Mtb infection (24).

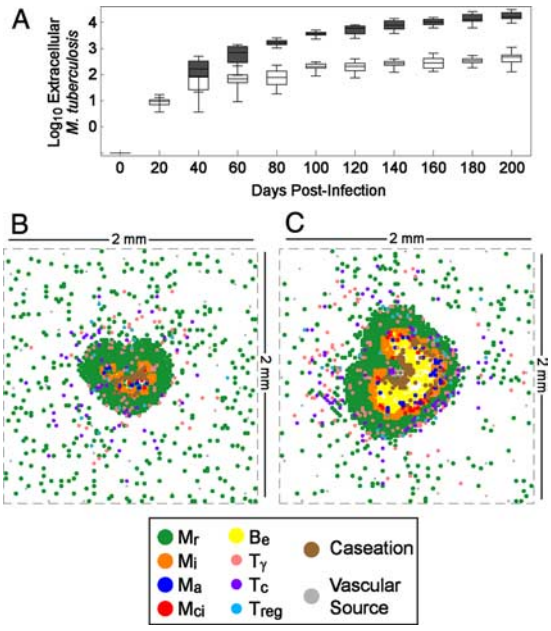

FIGURE 3. Simulated kinetics of extracellular Mtb and typical granuloma structures at 200 days postinfection in baseline control and TNF deletion scenarios. *A*, Box-whisker plots represent minimum, median, maximum, and interquartile range of bacterial numbers for 15 simulations each for the containment scenario (□) and lacking TNF (▨). *B*, Containment granuloma using the baseline set of parameters (Tables I–III). *C*, Irregular granuloma with uncontrolled bacterial growth resulting from lack of TNF in the simulation. B_e is extracellular mycobacteria. T_γ and T_c are proinflammatory and cytotoxic T cells, respectively. Parameters are as in Tables I–III, except for TNF deletion (where parameter $s_{TNF} = 0$).

Factors that substantially contribute to control of infection within the granuloma

To identify which parameters significantly contributed to control of Mtb infection within the granuloma, we performed a global uncertainty and sensitivity analysis, varying parameters in Tables I and II. Using the outcomes of this, we performed a sensitivity analysis to statistically determine which factors control bacterial numbers within the granuloma[6] (Fig. 4*A*). Approximately two-thirds of the simulations led to clearance of the infection. Some combinations of parameter values promote elimination of bacteria before granuloma formation due to apoptosis-induced killing and innate clearance by M_r (data not shown). The parameters that emerged as especially important were bacterial growth rates, T cell movement, and certain TNF-related effects. We then assessed the effects of these identified parameters on variables such as T cell functions, granuloma size, macrophage numbers, and level of caseation in the model (Table IV).

The analysis indicated that growth rates of intracellular and extracellular Mtb (α_{Bi} and α_{Be}, respectively) are positively correlated with increased bacterial numbers in the granuloma (4)

[6] This result differs slightly from our previous results in Segovia-Juarez et al. (38), which predicted that intracellular growth rates are transiently negatively correlated with extracellular Mtb numbers between days 30 and 150 postinfection. This discrepancy is due to a peak in chronically infected macrophage bursting in that model, which is not reproduced in this study, because we hold the initial number of macrophages constant. This allows uncertainty analysis to have identical initial conditions between different parameter sets.

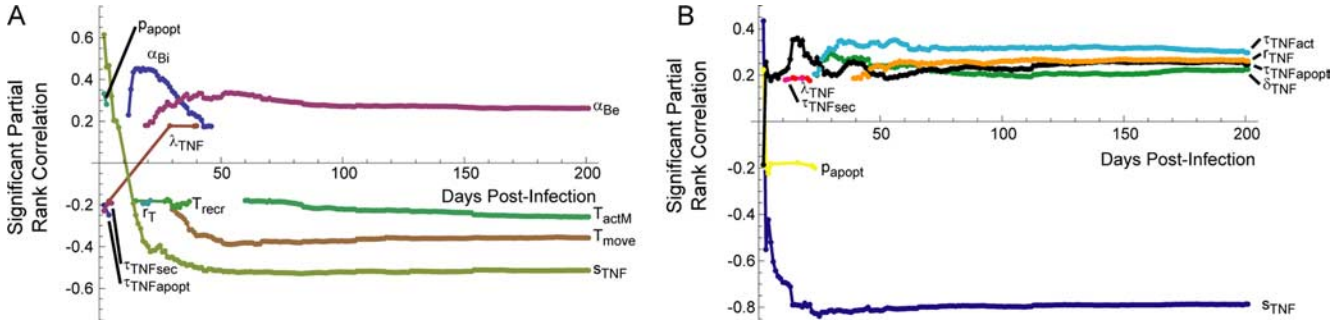

FIGURE 4. Correlation of mechanisms in the model with extracelluar bacterial load over the course of infection. Graphs depict significant partial rank correlations ($p < 0.01$). *A*, Global sensitivity analysis reveals four dominant parameters. *B*, TNF-focused sensitivity analysis predicts the contribution of individual TNF-related mechanisms over time. Non-TNF parameters are set equal to the baseline control scenario (Tables I–III) in *B*. α_{Be}, Extracellular Mtb growth rate; α_{Bi}, intracellular Mtb growth rate; p_{apopt}, probability of TNF-induced apoptosis in one 10-min interval; τ_{TNFact}, threshold for TNF-induced activation by macrophages; r_{MTNF}, effect of TNF on transendothelial migration; δ_{TNF}, rate of TNF degradation; $\tau_{TNFapopt}$, threshold for TNF-induced apoptosis by macrophages.

(Fig. 4*A*). This result suggests that the growth rate of mycobacteria is a virulence factor, consistent with the published data that more virulent clinical strains of Mtb grow more quickly in macrophages (53). A faster intracellular growth rate leads to increased secretion of TNF and chemokines early in infection (due to increased antigenic stimulation), and to increased T cell activity by 200 days postinfection (Table IV). However, the heightened immune response is apparently incapable of controlling the infection in the face of the increased bacterial growth rate. This is recapitulated in animal models, in which increased bacterial numbers result in increased inflammation and more T cell activation, but not necessarily better control of infection (54).

Not surprisingly, the probability (T_{move}) of a T cell moving to a location occupied by another cell (either a T cell or a macrophage) is significantly negatively correlated with bacterial levels (Fig. 4*A*). A microcompartment can hold either two T cells or a T cell and a macrophage, but not two T cells and a macrophage or more than one macrophage. At 200 days, an increase in the rate of T_{move} negatively impacts every measure in our model. In other words, a more tightly packed granuloma is more effective in controlling bacterial numbers, because this increases cell-cell interactions, leading to activation of infected macrophages by T cells.

As expected from the human and animal model data and our previous studies (17, 20), TNF is crucial to the outcome of infection at the level of the granuloma (Fig. 3). In this analysis, the overall rate of TNF production (s_{TNF}) was strongly negatively correlated with bacterial numbers (Fig. 4*A*), confirming the necessity for TNF in controlling infection. Increased TNF production from the beginning of infection resulted in clearance of infection in more than one-half of the simulations. The rate of TNF secretion strongly and negatively influences most variables in the model, particularly in the long-term (see Table IV), suggesting that the rate of TNF secretion from macrophages and T_γ cells (s_{TNF}) has a global regulatory role in the system, with a major impact on immune cell and bacterial populations.

Table IV. *Significant partial rank correlations between parameters identified in the Sensitivity Analysis in Fig. 4 and various granuloma outcome measures 20 and 200 days postinfection for several different outcome variables (column 1)*[a]

	α_{Bi}		α_{Be}		s_{TNF}		T_{move}	
	Day 20	Day 200	Day 20	Day 200	Day 20	Day 200	Day 20	Day 200
Outcome measure								
B_e	+++		+	+++	—	—		—
B_i	+++				—	—		—
Total T cells						—		—
T_γ						—		—
Secretor T_γ[b]		+++				–		–
T_c						—		—
T_{reg}						—		—
Total Macs					—	—		—
M_r					—	—		—
M_I					—	—		—
M_{ci}	+++	+			—	—		—
M_a		++				—		—
TNF	+				—	—		—
Chemokines	++				—	—		—
Caseation		+++				—		—
B_e growth rate	+++	+++			—	—		—
Granuloma size	ND[c]		ND[c]		ND[c]	—	ND[c]	—

[a] Parameter definitions are given in Tables I–III. Significant positive correlations: +++, $p < 0.0001$; ++, $p < 0.001$; +, $p < 0.01$. Significant negative correlations: – – –, $p < 0.0001$; – –, $p < 0.001$; -, $p < 0.01$.

[b] Number of T_γ cells actively secreting IFN-γ.

[c] ND, Not done due to relative lack of granuloma formation by day 20.

Table V. *Significant changes in granuloma variables at the final time point[a] for deletion and depletion of all TNF activity (All TNF), TNF-induced activation activity (Activation), and TNF-induced apoptosis activity (Apoptosis) vs the baseline control scenario[b]*

	All TNF		Activation		Apoptosis	
	Del (A)	Depl (B)	Del (C)	Depl (D)	Del (E)	Depl (F)
B_{tot}[3]	+++	+++	+++	+++	---	---
B_e	+++	+++	+++	+++	---	---
B_i	+++	+++			---	---
Total T cells						+
T_γ						+
"Secretor" T_γ[4]	++				--	-
T_c						+
T_{reg}						+
Total Macrophages			-	-		+
M_r					+	+++
M_i	+++	+++		+	---	---
M_{ci}	+++	+++			---	---
M_a			---	---		
TNF	---	---			+	++
Chemokines	+++	+++			+	++
Caseation	+++	+++	+++	+++	---	---
Granuloma Size	+++	+++			ND[5]	ND[5]

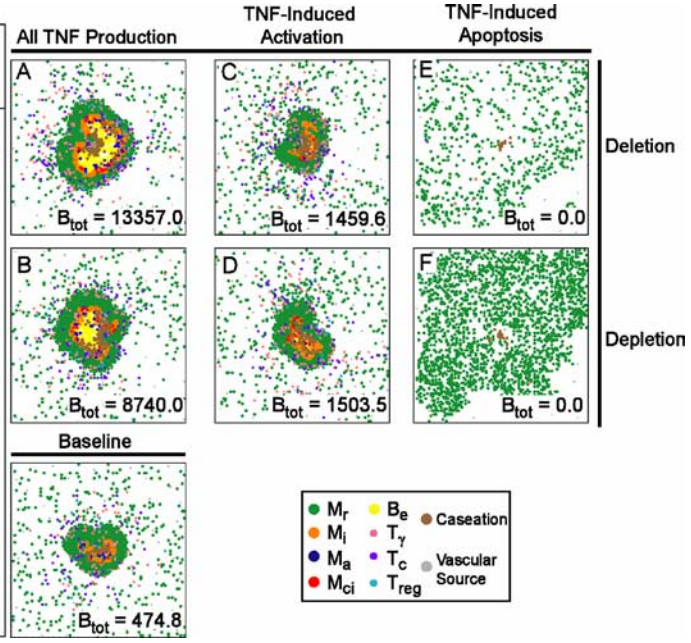

[a] Two hundred days postinfection (Activation), or the day when complete bacterial elimination occurs (Apoptosis).
[b] Representative granuloma structures for each deletion and depletion are shown. A full list of all simulated granulomas for ach deletion/depletion is given in Supplement 3. +, Denotes a higher variable value for the deletion or depletion than the control scenario; -, denotes a lower value. +++, $p < 0.0001$; ++, $p < 0.001$; +, $p < 0.01$. Significant negative correlations: ---, $p < 0.0001$; --, $p < 0.001$; -, $p < 0.01$.
[c] $B_{tot} = B_e + B_i$.
[d] Number of T_γ cells actively secreting IFN-γ.
[e] Nearly complete bacterial elimination prevented testing.

Contribution of individual TNF-dependent mechanisms to infection outcome

The original analysis confirmed a major role for TNF in control of the infection within the granuloma. In this model and in vivo, TNF has numerous functions, including inducing secretion of TNF and chemokines, activation of macrophages to a bactericidal state (in concert with IFN-γ), recruitment of cells, and apoptosis of macrophages. To assess the correlation of individual TNF-related functions with control of bacterial infection, we performed a focused sensitivity analysis, varying only the seven TNF parameters, with all other parameters at the values shown in Tables II and III.

This analysis (Fig. 4*B*) reveals positive correlations between extracellular Mtb numbers and four TNF-related parameters: τ_{TNFact} (threshold for TNF-induced activation by macrophages); $\tau_{TNFapopt}$ (threshold for TNF-induced apoptosis by macrophages); δ_{TNF} (rate of TNF degradation); and r_{TNF} (effect of TNF on cell recruitment via transendothelial migration). Not surprisingly, the rate of TNF secretion from macrophages and T_γ cells (s_{TNF}) is still the most significantly correlated mechanism (Fig. 4*B*). These results suggest that multiple TNF-dependent mechanisms contribute to the observed effect of TNF on bacterial control.

The role of individual TNF-dependent mechanisms in control of infection

To identify the contribution of each TNF-dependent mechanism individually to the outcome of infection at the granuloma level, we simulated deletion and depletion of each mechanism (both single and in combination).

Virtual deletion and depletion of TNF-related macrophage activation show significantly higher levels of extracellular bacteria and caseation, with lower numbers of activated macrophage and unchanged granuloma size (Table V; cf Supplement 3, Fig. S2 for all simulated granulomas). The granuloma structures resemble an intermediate between the tightly packed form of the baseline scenario and the irregular core observed with complete TNF deletion or depletion (see Fig. 3). Caseation is most likely increased because bacterial numbers increase, leading to more macrophage cell death (which contributes to caseation).

Deletion and depletion of TNF-induced secretion activity (Table VI) suggest different roles for this activity before and after T cell infiltration begins. Loss of secretion activity (that is, TNF-inducing TNF and chemokine production from macrophages) leads to higher levels of caseation and extracellular bacteria during a simulated deletion. No significant effects on these variables are observed during depletion, which has elevated intracellular bacteria and TNF/chemokines (compare Table VI, *E* and *F*). In contrast, during both deletion and depletion (Table VI, *C* and *D*), loss of TNF recruitment activity leads to a reduction of immune cells, indicating that this function of TNF is not infection stage specific.

When comparing infection initiated with 1 bacterium (above) with that of 15 bacteria as the inoculum, there are differences in the TNF analysis. While examining the role of each TNF activity in the higher inoculum scenario, we found that the effects of depleting TNF-induced secretion are not significant in the 15 bacteria case, as it was in the single bacterium scenario. This implies that aspects of TNF activities may be sensitive to the initial bacterial inoculum. We are exploring this dose-response topic further in a manuscript in preparation.

Is there a synergy or trade-off between TNF activities?

To determine the effects of interactions between specific TNF activities on granuloma structure, we performed virtual deletions and

Table VI. *Significant changes in granuloma variables at 200 days postinfection for deletion and depletion of all TNF activity (All TNF), TNF effects on cellular transendothelial migration activity (Recruitment), and TNF-induced secretion of chemokines/TNF activity (Secretion) vs the baseline control scenario*[a]

	All TNF		Recruitment		Secretion	
	Del (A)	Depl (B)	Del (C)	Depl (D)	Del (E)	Depl (F)
B_{tot}[2]	+++	+++			+	++
B_e	+++	+++			+	
B_i	+++	+++				++
Total T cells			--	--		
T_γ			--	--		
"Secretor" T_γ[3]	++					
T_c			-	---		
T_{reg}						
Total Macrophages				-		
M_r				-		
M_i	+++	+++			+	+
M_{ci}	+++	+++				
M_a						
TNF	---	---				+
Chemokines	+++		-			++
Caseation	+++	+++			+++	
Granuloma Size	+++	+++				

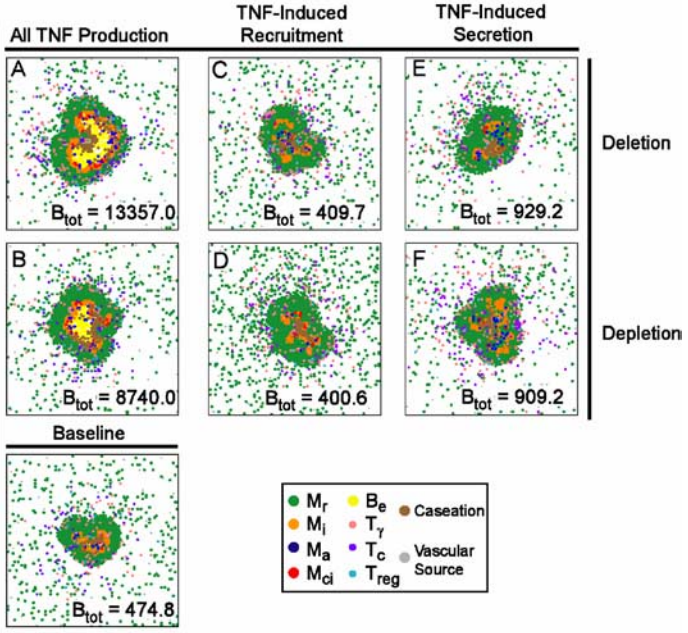

[a] Representative granuloma structures for each deletion and depletion are shown. A full list of all simulated granulomas for ach deletion/depletion is given in Supplement 3. +, Denotes a higher variable value for the deletion or depletion than the control scenario; -, denotes a lower value. +++, $p < 0.0001$; ++, $p < 0.001$; +, $p < 0.01$. Significant negative correlations: – – –, $p < 0.0001$; – –, $p < 0.001$; -, $p < 0.01$.

[b] $B_{tot} = B_e + B_i$.

[c] Number of T_γ cells actively secreting IFN-γ.

depletions of pairs and triplets of individual activities. In this section, we present results for TNF-dependent secretion, recruitment, and activation, deferring exploration of apoptosis activity to the section below.

Performing virtual double deletion/depletion of TNF-dependent recruitment and either secretion or activation activity results in the same outcome as either single depletion for secretion or activation (compare Fig. 5, *A* and *B*, with Tables V and VI). This suggests that TNF-dependent recruitment is not playing a major role in the control of infection at the level of the granuloma. In contrast, virtual double deletion/depletion with TNF-dependent activation and secretion yields results similar to deletion/depletion of all TNF activities in which the granuloma is larger in size, bacterial levels are increased, and there is increased caseation (compare Fig. 5*C* with Tables V and VI). A triple deletion/depletion of these three activities also results in poorly formed granulomas with high bacterial loads and caseation (Fig. 5, *D* and *H*). Together these results suggest that both activation and secretion activities of TNF contribute important and distinct roles to granuloma function, formation, and/or maintenance, and that TNF-dependent recruitment is

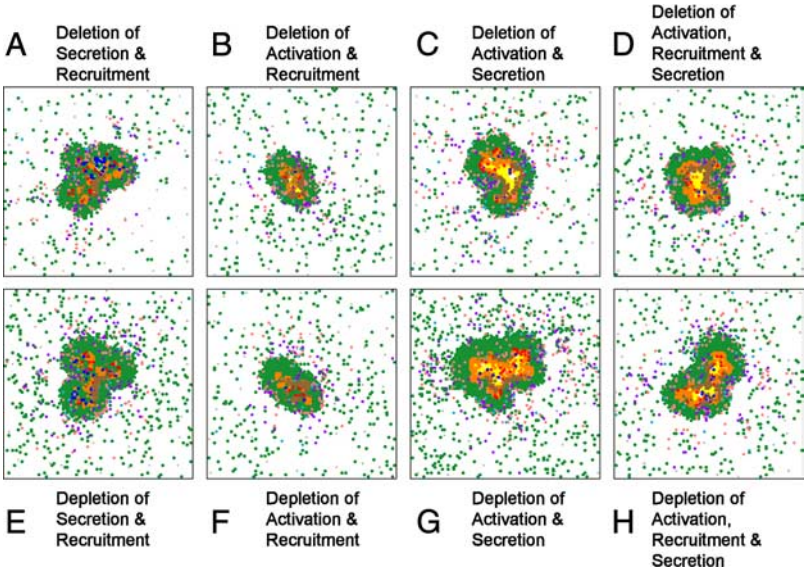

FIGURE 5. Representative double and triple deletions/depletions of TNF activities. Deletion of TNF-induced secretion and recruitment (*A*); activation and recruitment (*B*); activation and secretion (*C*); and activation, recruitment, and secretion (*D*). *E–H*, Analogous combinations of targeted TNF depletions. Structures for multiple replicates of each simulation, and for depletions of each combination at 100 days postinfection, are given in Supplement 3.[6]

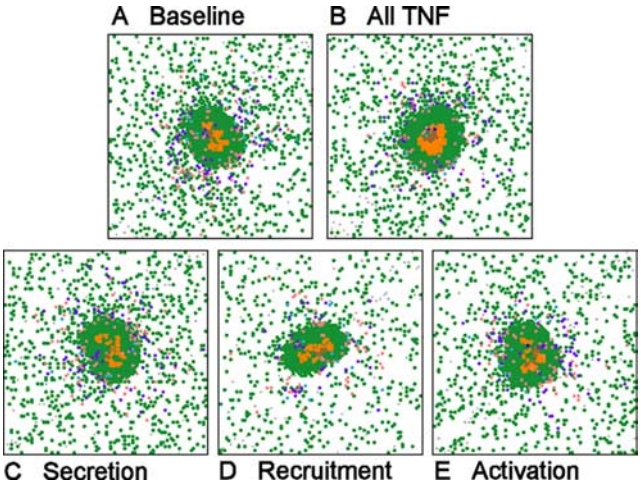

FIGURE 6. Characteristic granulomas resulting from holding total bacterial numbers fixed after day 100. Shown are as follows: baseline (*A*), virtual depletion of all TNF activities (*B*), virtual depletion of TNF secretion activity (*C*), TNF recruitment activity (*D*), and TNF activation activity (*E*).

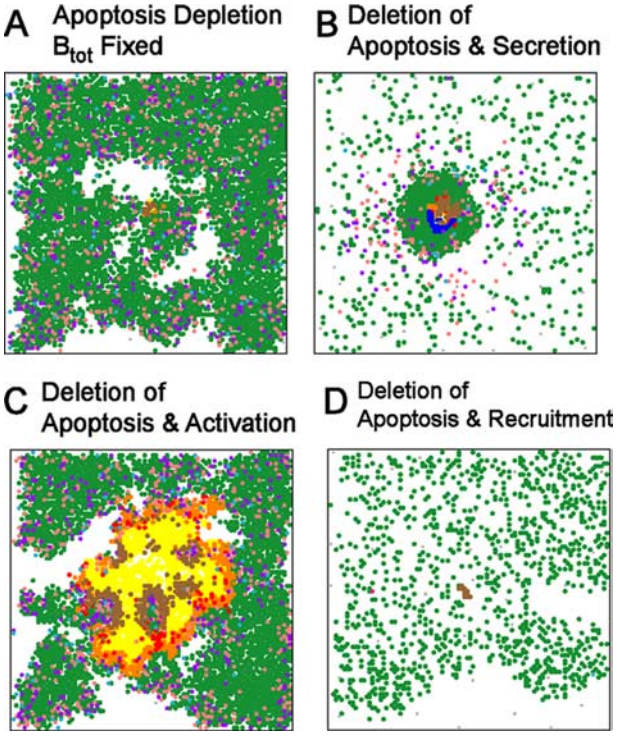

FIGURE 7. Effects of losing TNF-induced apoptosis activity on granuloma structures 200 days postinfection. *A*, Characteristic structures that are attainable under apoptosis depletion with total bacterial numbers held constant after day 100. *B*, Deletion of apoptosis and TNF-induced secretion. *C*, Deletion of both TNF-induced apoptosis and activation. *D*, Deletion of both TNF-induced apoptosis and recruitment. In the latter structures, continued bacterial growth after day 100 was permitted. A full list of apoptosis-related deletions is presented in Supplement 3.

not a significant factor. Supplement 3, Fig. S3, shows all simulated granulomas at day 200 for all combinations of deletions and depletions.

Granuloma structure

For many of the results obtained to date, it is difficult to distinguish the role of bacterial numbers vs TNF activity in driving the structure of the granuloma. To address this, we performed a simulation that is impossible to do in vivo, namely, to allow the granuloma to form and then to fix the total number of bacteria present (see *Materials and Methods* for more details). This allows us to isolate the effects of TNF without the contribution of changing bacterial numbers. Fig. 6 shows results of fixing the bacterial levels and performing virtual depletions performed at day 100 for the following: all TNF, secretion, recruitment, and activation activities, respectively. Depletion of TNF recruitment in these simulations did have an impact on the number of T cells at the site, and the granulomas were on average smaller (but not significantly so). However, the granuloma structures were not affected. In all other cases, depletion of the single TNF activities did not affect the shape or size of the granuloma once bacterial numbers were fixed. This suggests that bacterial load is the primary factor responsible for determining granuloma structure and shape.

Role of TNF-induced apoptosis

An unanticipated finding was that deletion and depletion of TNF-induced apoptosis result in effective clearance of bacteria ("Apoptosis" in Table V). At the time after all bacteria were cleared, there is disrupted granuloma structure with a robust increase in cell infiltration and TNF/chemokine production (Table V). Separate depletion of TNF-induced apoptosis activity from infected and uninfected macrophages shows that this phenomenon is primarily driven by uninfected macrophages, which constitute the largest macrophage subpopulation (data not shown). These data suggest that TNF-induced apoptosis of uninfected macrophages within the granuloma prevents excessive inflammation, but this leads to persistent Mtb infection.

To directly assess the contribution to granuloma structure, we fixed bacterial numbers at 100 days, as described above, and eliminated TNF-dependent apoptosis. We again observed the hyperinflammatory state described above (Fig. 7*A*). This supports a major role for uninfected macrophages driving granuloma structure. One possible explanation is that in the absence of apoptotic cell death of macrophages, induction of TNF at the site of infection continues to induce TNF in surrounding macrophages, forming a positive feedback loop, a process normally limited by TNF-induced apoptosis in this model.

To test this possibility, we performed virtual deletion or depletion of both apoptosis and TNF-induced secretion of both TNF and chemokines (Fig. 7*B*). Without secretion of TNF and chemokines, loss of apoptosis did not result in enhanced inflammation and resolution of infection, clearly demonstrating that the robust inflammatory response in the single deletion and depletion of apoptosis was dependent on TNF-mediated induction of TNF and chemokines from uninfected macrophages. This may be a feedback loop in which bacteria released by dying macrophages induce secretion of TNF, and higher subsequent levels of TNF and chemokines. Apoptosis of macrophages most likely prevents this TNF-induced cytokine/chemokine response by both reducing the bacteria released from macrophages and eliminating excess macrophages from the granuloma; these macrophages are the source of the cytokines and chemokines that influence the inflammatory response. Combining a loss of TNF-mediated apoptosis with loss of TNF-induced macrophage activation (Fig. 7*C*) results in substantially worse inflammation, but no clearance of bacteria, because macrophage activation is essential for Mtb killing. Deleting or depleting both apoptosis and TNF-mediated cell recruitment (Fig. 7*D*) is not different from the individually simulated apoptosis deletion and

depletion, indicating that the observed excess inflammation is not due to changes in total recruitment of cells to the lungs.

Discussion

TNF is clearly a central factor in control of Mtb infection. It has been repeatedly demonstrated in murine models that granuloma function, formation, and maintenance are dependent on TNF (24). However, TNF is a pleiotropic cytokine, and the relative contributions of its primary activities to the functional and structural characteristics of the granuloma have not been elucidated. The complex nature of TNF in the immune response to Mtb most likely accounts for the dramatic effects observed when neutralizing this cytokine in humans with latent Mtb infection (21) and in animal models (16, 19). The ABM of a tuberculous granuloma developed in this study is unique in its ability to address the roles of individual functions of TNF in granuloma formation and control of infection. The major findings from this study are as follows: 1) both TNF-induced macrophage activation and TNF-dependent secretion of chemokines and cytokines are crucial factors in control of infection within the granuloma; 2) TNF-induced apoptosis functions to reduce inflammation at the expense of impairing bacterial clearance; and 3) structural alterations in granuloma size and shape resulting from perturbation of TNF activity are directly driven by bacterial growth, and indirectly by TNF activities.

Our ABM of granuloma formation reproduces major features of infection by representing interactions of individual cell agents and molecular effectors with a representation of a growing mycobacterial population. This work was based on a previous model (38) with major extensions that include representations of TNF, a simple chemokine network, and distinct T cell subpopulations, including effector and regulatory cells. A baseline parameter set demonstrates bacterial control and variable granuloma structures, both of which are disrupted by virtual deletion or depletion of TNF. This sophisticated model allows for a spatial and temporal representation of events occurring during granuloma formation and function, allowing for exploration of this complex biological system in ways that are currently not tractable with experimental methods. A next logical step is to consider a three-dimensional spatial representation, and this may be important for making further predictions about elements within the system. In contrast, a three-dimensional granuloma model (55) gave similar results to our previous two-dimensional model (38), suggesting that the two-dimensional approach is sufficient to study many aspects of granuloma formation.

One further important simplification in our model is a reduction in the number of cell types to only those with well-characterized roles in Mtb granulomas. Multinucleate giant cells may modulate chemokine production (56) without taking up extracellular Mtb (57); dendritic cells are necessary for optimal antigenic stimulation of T cells (58, 59); foamy cells are dendritic-like cells (60) that may be a nutrient source for Mtb (61); B cells form ectopic germinal centers in Mtb-infected mouse lungs, with some role in containment (62). Each of these cell types may have important quantitative or qualitative roles, but are not sufficiently characterized to include in this model. Future work can easily incorporate these into the model when mechanistic information becomes available.

Our model provides the opportunity to study various combinations of effector functions controlled by TNF. Virtual deletion or depletion of each individual TNF-related function demonstrated that TNF-dependent macrophage activation was the primary factor involved in control of bacterial numbers, but that TNF-induced chemokine and TNF secretion also played a role in this process, probably by bringing macrophages and T cells close together in the granuloma, as well as producing more TNF in the granuloma. In contrast, loss of TNF-mediated recruitment, in which TNF acts on the vasculature to bring more cells into the lungs, had little effect on bacterial numbers, but resulted in recruitment of fewer immune cells. This is consistent with reduced recruitment in TNF-blockaded *Mycobacterium bovis* bacillus Calmette-Guerin infection in mice (63); lower virulence of bacillus Calmette-Guerin compared with Mtb may explain why complete loss of TNF activity did not cause a severe phenotype in that study.

Virtual elimination of both TNF-dependent macrophage activation and cytokine/chemokine secretion resulted in large granulomas with extensive caseation and lack of bacterial control that was essentially identical with the scenario of total loss of TNF, and was worse than loss of either function independently. In contrast, eliminating TNF-mediated recruitment had no additional detrimental effects when coupled with the loss of TNF-dependent macrophage activation or secretion. Thus, both macrophage activation and cytokine/chemokine secretion induced by TNF are important and distinct functions in control of bacterial numbers in the granuloma.

Based on data in the murine system, including our own data, it has been widely believed that TNF is the major factor that controls the actual formation, structure, and maintenance of a granuloma (17, 64). Humans treated with TNF-neutralizing drugs for inflammatory diseases have an increased incidence of reactivation TB. In an initial report (21), lung biopsies from a patient with disseminated TB due to TNF neutralization did not reveal granulomas, supporting the murine data. However, another human study (65) has indicated that granulomas are present in tuberculous lungs from TNF-neutralized patients, calling into question whether TNF is required for maintenance of granulomas. Indeed, data from our nonhuman primate model of TB also indicate that granulomas can form and be maintained even when TNF is neutralized (P. L. Lin and J. L. Flynn, submitted for publication).

The current virtual model provides an opportunity to test the functions of TNF that are related to granuloma function, formation, and structure. The flexibility of this model, compared with in vivo systems, allows us to hold the bacterial numbers steady while varying other parameters. This provides an opportunity to distinguish between effects of granuloma structure that are due to bacterial numbers or to TNF-dependent factors. In fact, when bacterial numbers cannot increase as a result of TNF depletion, granuloma structure is essentially unaffected by loss of TNF-dependent factors. This suggests that bacterial numbers are a driving force in the aberrations in granuloma formation and maintenance due to loss of TNF. This does not negate a role for TNF in the formation and maintenance of granulomas, but instead suggests that bacterial numbers play a greater role in this than previously believed.

One surprising finding was that deletion and depletion of TNF-induced apoptosis result in effective clearance of bacteria. Simulations predicted disrupted granuloma structure and increased cell infiltration and TNF/chemokine production in this case. Virtual depletion of TNF-induced apoptosis activity from infected or uninfected macrophages demonstrated that this phenomenon is primarily driven by uninfected macrophages. Comparing dual and single depletions, as well as the fixed bacterial numbers simulations, it became clear that the increased inflammation observed in the absence of apoptosis was due to TNF-induced secretion of chemokines and TNF from uninfected macrophages. This function of TNF enhances bacterial clearance, but can lead to excessive pathology. Thus, a role for TNF-induced apoptosis seems to be

control of pathology at the expense of bacterial clearance. This provides evidence that the outcome of infection in any one granuloma is a balance of different factors, including TNF-induced functions. This result may differ if certain anti-inflammatory cytokines such as IL-10 were included in the model, which could modulate the effects of TNF; this possibility has been proposed previously (66).

The size of the initial bacterial inoculum may have some effects on progression and containment of Mtb infection, particularly in cases with immunological deficiencies (e.g., Ref. 67). We explored the effects of increasing the bacterial load in the first infected macrophage from 1 bacterium to 15. Cell and bacterial kinetics were different preceding T cell infiltration at 20 days postinfection, but became very similar after (data not shown). The primary difference in dose as it relates to TNF activities is for TNF-induced secretion of chemokines and TNF. For the low inoculum, depleting this activity significantly affected aspects of the granuloma (Table VI), in which for the higher inoculum, no significant effects for the depletion were observed (data not shown). A very high inoculum, above the small range we tested in this study, would most likely have dramatic effects on the outcome of infection, as demonstrated in our previous studies (6, 20), although the effect may not manifest at the level of a single granuloma. We have a manuscript in preparation exploring the role of initial dose in a more detailed fashion.

In this work, we have used an advanced mathematical modeling approach to identify the relative contribution of different TNF-dependent activities in granuloma formation and function. Model results predicted mechanisms involved in control of both bacterial numbers within the granuloma as well as inflammation. These mechanisms can now serve as putative targets for vaccine and treatment strategies. The approach applied in this study contributes groundwork for the use of computational approaches in identifying biological pathways that can be targeted for modulation of TB.

Acknowledgments

We thank members of J.C.J.R.'s PhD thesis committee (Gary Huffnagle, Jennifer Linderman, Alex Ninfa, and Joel Swanson); Shlomo Ta'asan and other members of the Center for Modeling Pulmonary Immunity; P. Ling Lin; and Steven Kunkel and Simeone Marino for helpful comments.

Disclosures

The authors have no financial conflict of interest.

References

1. Flynn, J. L., and J. Chan. 2001. Immunology of tuberculosis. *Annu. Rev. Immunol.* 19: 93–129.
2. Ridley, M., C. Heather, I. Brown, and D. Willoughby. 1983. Experimental epithelioid cell granulomas tubercle formation and immunological competence: an ultrastructural analysis. *J. Pathol.* 141: 97–112.
3. Emile, J. F., N. Patey, F. Altare, S. Lamhamedi, E. Jouanguy, F. Boman, J. Quillard, M. Lecomte-Houcke, O. Verola, J. F. Mousnier, et al. 1997. Correlation of granuloma structure with clinical outcome defines two types of idiopathic disseminated BCG infection. *J. Pathol.* 181: 25–30.
4. Lin, P. L., S. Pawar, A. Myers, A. Pegu, C. Fuhrman, T. A. Reinhart, S. V. Capuano, E. Klein, and J. L. Flynn. 2006. Early events in *Mycobacterium tuberculosis* infection in cynomolgus macaques. *Infect. Immun.* 74: 3790–3803.
5. Hoebe, K., E. Janssen, and B. Beutler. 2004. The interface between innate and adaptive immunity. *Nat. Immunol.* 5: 971–974.
6. Sud, D., C. Bigbee, J. L. Flynn, and D. E. Kirschner. 2006. Contribution of $CD8^+$ T cells to control of *Mycobacterium tuberculosis* infection. *J. Immunol.* 176: 4296–4314.
7. Vignali, D., L. Collison, and C. Workman. 2008. How regulatory T cells work. *Nat. Rev. Immunol.* 8: 523–532.
8. Mason, C. M., E. Porretta, P. Zhang, and S. Nelson. 2007. $CD4^+CD25^+$ transforming growth factor-producing T cells are present in the lung in murine tuberculosis and may regulate the host inflammatory response. *Clin. Exp. Immunol.* 148: 537–545.
9. Guyot-Revol, V., J. A. Innes, S. Hackforth, T. Hinks, and A. Lalvani. 2006. Regulatory T cells are expanded in blood and disease sites in patients with tuberculosis. *Am. J. Respir. Crit. Care Med.* 173: 803–810.
10. Ordway, D., M. Henao-Tamayo, M. Harton, G. Palanisamy, J. Troudt, C. Shanley, R. Basaraba, and I. Orme. 2007. The hypervirulent *Mycobacterium tuberculosis* strain HN878 induces a potent TH1 response followed by rapid down-regulation. *J. Immunol.* 179: 522–531.
11. Roberts, T., N. Beyers, A. Aguirre, and G. Walzl. 2007. Immunosuppression during active tuberculosis is characterized by decreased interferon-γ production and CD25 expression with elevated forkhead box P3, transforming growth factor-β, and interleukin-4 mRNA levels. *J. Infect. Dis.* 195: 870–878.
12. Asano, M., M. Toda, N. Sakaguchi, and S. Sakaguchi. 1996. Autoimmune disease as a consequence of developmental abnormality of a T cell subpopulation. *J. Exp. Med.* 184: 387–396.
13. Sakaguchi, S., N. Sakaguchi, M. Asano, M. Itoh, and M. Toda. 1995. Immunologic self-tolerance maintained by activated T cells expressing IL-2 receptor α-chains (CD25): breakdown of a single mechanism of self-tolerance causes various autoimmune diseases. *J. Immunol.* 155: 1151–1164.
14. Thornton, A. M., and E. M. Shevach. 1998. $CD4^+CD25^+$ immunoregulatory T cells suppress polyclonal T cell activation in vitro by inhibiting interleukin 2 production. *J. Exp. Med.* 188: 287–296.
15. Baatar, D., P. Olkhanud, K. Sumitomo, D. Taub, R. Gress, and A. Biragyn. 2007. Human peripheral blood T regulatory cells (Tregs), functionally primed $CCR4^+$ Tregs and unprimed $CCR4^-$ Tregs, regulate effector T cells using FasL. *J. Immunol.* 178: 4891–4900.
16. Flynn, J. L., M. M. Goldstein, J. Chan, K. J. Triebold, K. Pfeffer, C. J. Lowenstein, R. Schreiber, T. W. Mak, and B. R. Bloom. 1995. Tumor necrosis factor-α is required in the protective immune response against *Mycobacterium tuberculosis* in mice. *Immunity* 2: 561–572.
17. Bean, A., D. Roach, H. Briscoe, M. France, H. Korner, J. Sedgwick, and W. Britton. 1999. Structural deficiencies in granuloma formation in TNF gene-targeted mice underlie the heightened susceptibility to aerosol *Mycobacterium tuberculosis* infection, which is not compensated for by lymphotoxin. *J. Immunol.* 162: 3504–3511.
18. Bekker, L. G., S. Freeman, P. J. Murray, B. Ryffel, and G. Kaplan. 2001. TNF-α controls intracellular mycobacterial growth by both inducible nitric oxide synthase-dependent and inducible nitric oxide synthase-independent pathways. *J. Immunol.* 166: 6728–6734.
19. Mohan, V. P., C. A. Scanga, K. Yu, H. M. Scott, K. E. Tanaka, E. Tsang, M. M. Tsai, J. L. Flynn, and J. Chan. 2001. Effects of tumor necrosis factor α on host immune response in chronic persistent tuberculosis: possible role for limiting pathology. *Infect. Immun.* 69: 1847–1855.
20. Marino, S., D. Sud, H. Plessner, P. L. Lin, J. Chan, J. L. Flynn, and D. E. Kirschner. 2007. Differences in reactivation of tuberculosis induced from anti-TNF treatments are based on bioavailability in granulomatous tissue. *PLoS Comput. Biol.* 3: 1909–1924.
21. Keane, J., S. Gershon, R. P. Wise, E. Mirabile-Levens, J. Kasznica, W. D. Schwieterman, J. N. Siegel, and M. M. Braun. 2001. Tuberculosis associated with infliximab, a tumor necrosis factor α-neutralizing agent. *N. Engl. J. Med.* 345: 1098–1104.
22. Winthrop, K. L. 2006. Risk and prevention of tuberculosis and other serious opportunistic infections associated with the inhibition of tumor necrosis factor. *Nat. Clin. Pract. Rheumatol.* 2: 602–610.
23. Zhou, Z., M. C. Connell, and D. J. Macewan. 2007. TNFR1-induced NF-κB, but not ERK, p38MAPK or JNK activation, mediates TNF-induced ICAM-1 and VCAM-1 expression on endothelial cells. *Cell. Signal.* 19: 1238–1248.
24. Algood, H. M., P. L. Lin, and J. L. Flynn. 2005. Tumor necrosis factor and chemokine interactions in the formation and maintenance of granulomas in tuberculosis. *Clin. Infect. Dis.* 41(Suppl. 3): S189–S193.
25. Roach, D., A. Bean, C. Demangel, M. France, H. Briscoe, and W. Britton. 2002. TNF regulates chemokine induction essential for cell recruitment, granuloma formation, and clearance of mycobacterial infection. *J. Immunol.* 168: 4620–4627.
26. Van Buul, J., and P. Hordijk. 2004. Signaling in leukocyte transendothelial migration. *Arterioscler. Thromb. Vasc. Biol.* 24: 824–833.
27. Stein, J., and C. Nombela-Arrieta. 2005. Chemokine control of lymphocyte trafficking: a general overview. *Immunology* 116: 1–12.
28. Flesch, I., and S. Kaufmann. 1987. Mycobacterial growth inhibition by interferon-γ-activated bone marrow macrophages and differential susceptibility among strains of *Mycobacterium tuberculosis*. *J. Immunol.* 138: 4408–4413.
29. Flesch, I. E., and S. H. Kaufmann. 1990. Activation of tuberculostatic macrophage functions by γ interferon, interleukin-4, and tumor necrosis factor. *Infect. Immun.* 58: 2675–2677.
30. Rook, G. A., J. Steele, M. Ainsworth, and B. R. Champion. 1986. Activation of macrophages to inhibit proliferation of *Mycobacterium tuberculosis*: comparison of the effects of recombinant γ-interferon on human monocytes and murine peritoneal macrophages. *Immunology* 59: 333–338.
31. Laster, S. M., J. G. Wood, and L. R. Gooding. 1988. Tumor necrosis factor can induce both apoptic and necrotic forms of cell lysis. *J. Immunol.* 141: 2629–2634.
32. Keane, J., M. K. Balcewicz-Sablinska, H. G. Remold, G. L. Chupp, B. B. Meek, M. J. Fenton, and H. Kornfeld. 1997. Infection by *Mycobacterium tuberculosis* promotes human alveolar macrophage apoptosis. *Infect. Immun.* 65: 298–304.
33. Mohan, K., Z. Ding, J. Hanly, and T. B. Issekutz. 2002. IFN-γ-inducible T cell α chemoattractant is a potent stimulator of normal human blood T lymphocyte transendothelial migration: differential regulation by IFN-γ and TNF-α. *J. Immunol.* 168: 6420–6428.
34. Kristensen, N. N., M. Gad, A. R. Thomsen, B. Lu, C. Gerard, and M. H. Claesson. 2006. CXC chemokine receptor 3 expression increases the disease-inducing potential of $CD4^+$ $CD25^-$ T cells in adoptive transfer colitis. *Inflamm. Bowel Dis.* 12: 374–381.

35. Valente, A. J., D. T. Graves, C. E. Vialle-Valentin, R. Delgado, and C. J. Schwartz. 1988. Purification of a monocyte chemotactic factor secreted by nonhuman primate vascular cells in culture. *Biochemistry* 27: 4162–4168.
36. Peters, W., J. G. Cyster, M. Mack, D. Schlöndorff, A. J. Wolf, J. D. Ernst, and I. F. Charo. 2004. CCR2-dependent trafficking of F4/80^{dim} macrophages and CD11c$^{dim/intermediate}$ dendritic cells is crucial for T cell recruitment to lungs infected with *Mycobacterium tuberculosis*. *J. Immunol.* 172: 7647–7653.
37. Yurchenko, E., M. Tritt, V. Hay, E. Shevach, Y. Belkaid, and C. Piccirillo. 2006. CCR5-dependent homing of naturally occurring CD4$^+$ regulatory T cells to sites of *Leishmania major* infection favors pathogen persistence. *J. Exp. Med.* 203: 2451–2460.
38. Segovia-Juarez, J. L., S. Ganguli, and D. Kirschner. 2004. Identifying control mechanisms of granuloma formation during *M. tuberculosis* infection using an agent-based model. *J. Theor. Biol.* 231: 357–376.
39. Krombach, F., S. Munzing, A. M. Allmeling, J. T. Gerlach, J. Behr, and M. Dorger. 1997. Cell size of alveolar macrophages: an interspecies comparison. *Environ. Health Perspect.* 105(Suppl. 5): 1261–1263.
40. Sadek, M. I., E. Sada, Z. Toossi, S. K. Schwander, and E. A. Rich. 1998. Chemokines induced by infection of mononuclear phagocytes with mycobacteria and present in lung alveoli during active pulmonary tuberculosis. *Am. J. Respir. Cell Mol. Biol.* 19: 513–521.
41. Brice, G. T., N. L. Graber, S. L. Hoffman, and D. L. Doolan. 2001. Expression of the chemokine MIG is a sensitive and predictive marker for antigen-specific, genetically restricted IFN-γ production and IFN-γ-secreting cells. *J. Immunol. Methods* 257: 55–69.
42. Kang, S. G., R. J. Piniecki, H. Hogenesch, H. W. Lim, E. Wiebke, S. E. Braun, S. Matsumoto, and C. H. Kim. 2007. Identification of a chemokine network that recruits FoxP3$^+$ regulatory T cells into chronically inflamed intestine. *Gastroenterology* 132: 966–981.
43. Iijima, W., H. Ohtani, T. Nakayama, Y. Sugawara, E. Sato, H. Nagura, O. Yoshie, and T. Sasano. 2003. Infiltrating CD8$^+$ T cells in oral lichen planus predominantly express CCR5 and CXCR3 and carry respective chemokine ligands RANTES/CCL5 and IP-10/CXCL10 in their cytolytic granules: a potential self-recruiting mechanism. *Am. J. Pathol.* 163: 261–268.
44. Staruch, M. J., R. Camacho, and F. J. Dumont. 1998. Distinctive calcineurin-dependent (FK506-sensitive) mechanisms regulate the production of the CC chemokines macrophage inflammatory protein (MIP)-1α, MIP-1β, and RANTES vs IL-2 and TNF-α by activated human T cells. *Cell. Immunol.* 190: 121–131.
45. O'Brien, A. D., T. J. Standiford, P. J. Christensen, S. E. Wilcoxen, and R. Paine. 1998. Chemotaxis of alveolar macrophages in response to signals derived from alveolar epithelial cells. *J. Lab. Clin. Med.* 131: 417–424.
46. Tan, J., B. Deleuran, B. Gesser, H. Maare, M. Deleuran, C. G. Larsen, and K. Thestrup-Pedersen. 1995. Regulation of human T lymphocyte chemotaxis in vitro by T cell-derived cytokines IL-2, IFN-γ, IL-4, IL-10, and IL-13. *J. Immunol.* 154: 3742–3752.
47. Van Furth, R., M. C. Diesselhoff-den Dulk, and H. Mattie. 1973. Quantitative study on the production and kinetics of mononuclear phagocytes during an acute inflammatory reaction. *J. Exp. Med.* 138: 1314–1330.
48. Sprent, J. 1993. Lifespans of naive, memory and effector lymphocytes. *Curr. Opin. Immunol.* 5: 433–438.
49. Lazarevic, V., D. Nolt, and J. L. Flynn. 2005. Long-term control of *Mycobacterium tuberculosis* infection is mediated by dynamic immune responses. *J. Immunol.* 175: 1107–1117.
50. Francis, K., and B. O. Palsson. 1997. Effective intracellular communication distances are determined by the relative time constants for cyto/chemokine secretion and diffusion. *Proc. Natl. Acad. Sci. USA* 94: 12258–12262.
51. Marino, S., I. Hogue, C. Ray, and D. Kirschner. 2008. A methodology for performing global uncertainty and sensitivity analysis in systems biology. *J. Theor. Biol.* 254: 178–196.
52. Ulrichs, T., G. A. Kosmiadi, V. Trusov, S. Jörg, L. Pradl, M. Titukhina, V. Mishenko, N. Gushina, and S. H. Kaufmann. 2004. Human tuberculous granulomas induce peripheral lymphoid follicle-like structures to orchestrate local host defense in the lung. *J. Pathol.* 204: 217–228.
53. Theus, S., K. Eisenach, N. Fomukong, R. F. Silver, and M. D. Cave. 2007. Beijing family *Mycobacterium tuberculosis* strains differ in their intracellular growth in THP-1 macrophages. *Int. J. Tuberc. Lung Dis.* 11: 1087–1093.
54. Flynn, J. L. 2006. Lessons from experimental *Mycobacterium tuberculosis* infections. *Microbes Infect.* 8: 1179–1188.
55. Warrender, C., S. Forrest, and F. Koster. 2006. Modeling intercellular interactions in early *Mycobacterium* infection. *Bull. Math. Biol.* 68: 2233–2261.
56. Zhu, X. W., and J. S. Friedland. 2006. Multinucleate giant cells and the control of chemokine secretion in response to *Mycobacterium tuberculosis*. *Clin. Immunol.* 120: 10–20.
57. Lay, G., Y. Poquet, P. Salek-Peyron, M. P. Puissegur, C. Botanch, H. Bon, F. Levillain, J. L. Duteyrat, J. F. Emile, and F. Altare. 2007. Langhans giant cells from *M. tuberculosis*-induced human granulomas cannot mediate mycobacterial uptake. *J. Pathol.* 211: 76–85.
58. Uehira, K., R. Amakawa, T. Ito, K. Tajima, S. Naitoh, Y. Ozaki, T. Shimizu, K. Yamaguchi, Y. Uemura, H. Kitajima, et al. 2002. Dendritic cells are decreased in blood and accumulated in granuloma in tuberculosis. *Clin. Immunol.* 105: 296–303.
59. Giri, P., and J. Schorey. 2008. Exosomes derived from *M. bovis* BCG infected macrophages activate antigen-specific CD4$^+$ and CD8$^+$ T cells in vitro and in vivo. *PLoS ONE* 3: e2461.
60. Ordway, D., M. Henao-Tamayo, I. M. Orme, and M. Gonzalez-Juarrero. 2005. Foamy macrophages within lung granulomas of mice infected with *Mycobacterium tuberculosis* express molecules characteristic of dendritic cells and anti-apoptotic markers of the TNF receptor-associated factor family. *J. Immunol.* 175: 3873–3881.
61. Peyron, P., J. Vaubourgeix, Y. Poquet, F. Levillain, C. Botanch, F. Bardou, M. Daffé, J. F. Emile, B. Marchou, P. J. Cardona, et al. 2008. Foamy macrophages from tuberculous patients' granulomas constitute a nutrient-rich reservoir for *M. tuberculosis* persistence. *PLoS Pathog.* 4(11): e1000204.
62. Maglione, P. J., J. Xu, and J. Chan. 2007. B cells moderate inflammatory progression and enhance bacterial containment upon pulmonary challenge with *Mycobacterium tuberculosis*. *J. Immunol.* 178: 7222–7234.
63. Egen, J., A. Rothfuchs, C. Feng, N. Winter, A. Sher, and R. Germain. 2008. Macrophage and T cell dynamics during the development and disintegration of mycobacterial granulomas. *Immunity* 28: 271–284.
64. Chakravarty, S. D., G. Zhu, M. C. Tsai, V. P. Mohan, S. Marino, D. E. Kirschner, L. Huang, J. Flynn, and J. Chan. 2008. Tumor necrosis factor blockade in chronic murine tuberculosis enhances granulomatous inflammation and disorganizes granulomas in the lungs. *Infect. Immun.* 76: 916–926.
65. Iliopoulos, A., K. Psathakis, S. Aslanidis, L. Skagias, and P. Sfikakis. 2006. Tuberculosis and granuloma formation in patients receiving anti-TNF therapy. *Int. J. Tuberc. Lung Dis.* 10: 588–590.
66. Garcia-Ramallo, E., T. Marques, N. Prats, J. Beleta, S. L. Kunkel, and N. Godessart. 2002. Resident cell chemokine expression serves as the major mechanism for leukocyte recruitment during local inflammation. *J. Immunol.* 169: 6467–6473.
67. Scott, H. M., and J. L. Flynn. 2002. *Mycobacterium tuberculosis* in chemokine receptor 2-deficient mice: influence of dose on disease progression. *Infect. Immun.* 70: 5946–5954.